ICSES 2010 - THE INTERNATIONAL CONFERENCE ON SIGNALS AND ELECTRONIC SYSTEMS,
GLIWICE, POLAND, SEPTEMBER 7 - 10, 2010.

The Concept of CMOS OOK Transmitter Using Low Voltage Self-Oscillating Active Inductor

Grzegorz Szczepkowski*, John Dooley†, Ronan Farrell‡
CTVR - The Telecommunication Research Centre
National University of Ireland Maynooth
Email: {*gszczepkowski, †jdooley, ‡rfarrell}@eeng.nuim.ie

***Abstract*—This paper presents a low voltage, On-Off Keying (OOK) CMOS integrated transmitter for ISM 434 MHz biomedical applications using a concept of a novel self-oscillating (degenerated) active inductor. A thorough theoretical analysis of the oscillator is presented, together with simulated results using UMC 90 nm 1P9M RF process libraries. The proposed oscillator achieves an average phase noise of -93 dBc/Hz at 1 MHz offset from 434 MHz carrier frequency, with a relative tuning range of 26% to compensate for process variations. The transmitter allows modulation speeds up to 100 Mbps with RF output power of -4 dBm to 50 Ω load from 1 V power supply.**

I. INTRODUCTION

On-Off Keying (OOK) is historically the oldest type of electronic modulation, dating back to nineteenth century and wire telegraphy. Although simple, OOK allows transmission of digital signals with relative ease thus it has become a popular choice for biomedical applications [1]–[3]. Fig. 1 presents a generic model of such a transmitter, where continuous wave from signal generator is connected to the antenna through a digitally controlled switch. Information is encoded in a form of pulsed version of oscillator signal at carrier frequency. To minimise power dissipation, the OOK transmitter should not consume any energy during off state, which in turn, requires a fast transition times to support modulation with high data rates.

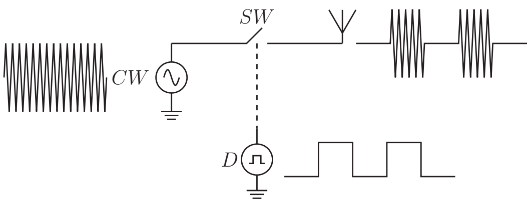

Fig. 1. Generic architecture of OOK transmitter.

This paper presents a complete OOK transmitter architecture able to achieve fast switching speeds due to the use of a novel low-power self-oscillating active inductor resonator. Low power consumption is achieved due to the use of the proposed technique of passive compensation using a RC phase shifter rather than a standard approach using an external active negative resistor. The paper is organized as follows. Section II describes the oscillator circuit with small signal parameters, oscillation criteria, large signal behavior and phase noise properties. Section III contains a complete transmitter architecture consisting of oscillator core, bias network, three stage buffer amplifier and switches. Section IV presents thorough simulation results of the circuit. Finally, the conclusions drawn from this work are presented.

II. DEGENERATED ACTIVE INDUCTOR OSCILLATOR

A. Circuit description

Moulding [4] observed that in gyrator based resonators, transconductance amplifiers generate additional negative conductance at high frequencies, due to a finite resistive losses and a parasitic capacitances of transistors and biasing networks. If not sufficiently suppressed, the effect of these parasitic phase shifters causes resonator peaking or instability [5]. By approaching this problem from a different perspective, the unfavorable instability effects of circuit parasitics, create a negative resistance LC oscillator, without the use of any additional active circuit. As transistor parasitics are generally hard to control, lumped phase lag networks can be used instead, while transconductor non-idealities are kept minimal at the frequency of interest.

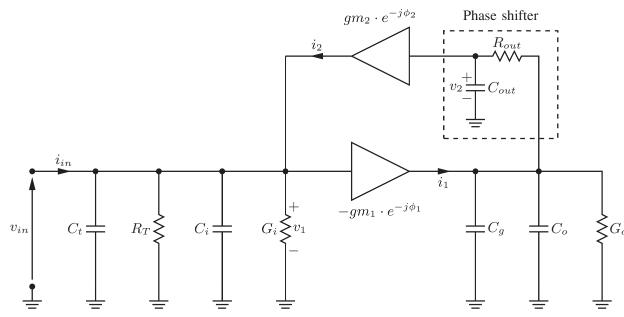

Fig. 2. Non-ideal degenerated active inductor resonator.

Fig. 2 depicts a degenerated gyrator tank with a single RC phase shifter at the output port of the active inductor. This design choice is not arbitrary. Two RC circuits would double the noise of a single phase shifter. If a single RC network is used at the input node, an observed negative resistance is more sensitive to frequency changes and has smaller inductive bandwidth than in the case of the chosen solution.

Components G_i and G_o represent total conductances at input and output nodes and consists of resistive losses of transconductors as well as a real part of input/output admittances of the amplifiers. Similarly, C_i and C_o characterise total node capacitances due to reactive parasitics. Respectively, R_T and C_t represent the parallel resistance and capacitance of the resonator originating from additional components connected to the gyrator (output buffer, for example). The phase shifter required for negative resistance generation is achieved by using R_{out} and C_{out}. Phase shifts of both transconductors, denoted by ϕ_1 and ϕ_2, are assumed to be negligible at sub-GHz frequencies. The input admittance of the proposed active resonator with output shifter can be found from

$$y_{in}(j\omega) = \frac{1}{R_T} + G_i + G_{pdg}(\omega) + j\omega C_T + \frac{1}{j\omega L_{pdg}(\omega)} \quad (1)$$

where

$$G_{pdg}(\omega) = \frac{gm_1 gm_2}{C_G \left(\omega_{z1} - \frac{\omega^2}{\omega_{z2}}\right)\left(1 + \frac{\omega^2 \omega_{z2}^2}{\left(\omega_{z1}\omega_{z2} - \omega^2\right)^2}\right)} \quad (2)$$

$$L_{pdg}(\omega) = \frac{C_G}{gm_1 gm_2}\left(1 + \frac{\left(\omega_{z1}\omega_{z2} - \omega^2\right)^2}{\omega^2 \omega_{z2}^2}\right) \quad (3)$$

$$(4)$$

and

$$C_T = C_t + C_i \quad (5)$$

$$C_G = C_g + C_o + C_{out}(1 + R_{out}G_o) \quad (6)$$

$$\omega_{z1} = \frac{G_o}{C_G} \quad (7)$$

$$\omega_{z2} = \frac{C_G}{\left(C_g + C_o\right) C_{out} R_{out}} \quad (8)$$

Equation (1) consists of four terms: input conductance, total tank capacitance, simulated parallel inductance $L_{pdg}(\omega)$ and an additional conductance $G_{pdg}(\omega)$ with a negative factor. Note that, both simulated inductance and negative conductance depend on frequency, bias conditions, phase shifter components and circuit parasitics.

B. Oscillation criteria

In general, the criteria for oscillation of any negative resistance oscillator are divided into amplitude and phase conditions, as in the case of Barkhausen criteria for feedback oscillators [6]. The amplitude condition enables calculation of parameter values for which total conductance (or resistance) of the resonator is zero. Similarly, a phase condition reveals circuit parameters for which total susceptance (or reactance) of the tank is zero.

Both conditions are found directly from (1). Results can be simplified, assuming that resonator losses are dominated by a gyrator input losses $G_i + 1/R_T \approx G_i$. In two transistor gyrators, where both amplifiers have the same gm and $gm \gg g_{out}$, generally $G_i \approx gm$ is observed. In this case, the amplitude condition is approximately equal to

$$gm + C_G\left(\omega_{z1} - \frac{\omega^2}{\omega_{z2}}\right)\left(1 + \frac{\omega^2\omega_{z2}^2}{\left(\omega_{z1}\omega_{z2} - \omega^2\right)^2}\right) = 0 \quad (9)$$

The phase condition reveals the resonant frequency of the circuit by finding the real and positive root of $\Im\{y_{in}(j\omega)\} = 0$ from (1)

$$\omega_0 = \frac{\sqrt{2}}{2}\omega_{z2}\sqrt{\sqrt{1 - 4\frac{\omega_{z1}}{\omega_{z2}} + 4\frac{gm_1 gm_2}{\omega_{z2}^2 C_G C_T}} + 2\frac{\omega_{z1}}{\omega_{z2}} - 1} \quad (10)$$

where corresponding parameters are defined by (5)-(8).

C. Large signal behavior

In the degenerated active inductor, large signals cause harmonic compression of negative conductance $G_{pdg}(\omega)$ at fundamental frequency due to odd-order harmonics. During oscillation build-up, the circuit starts to diverge from small signal behavior and, at a certain level, the amplitude condition is violated. When this happens, the resonator becomes dissipative and the oscillation amplitude reaches a maximum. It is observed that signal amplitude and distortion are proportional to the magnitude of negative conductance margin required to start oscillations. If a start-up margin is low, then the signal amplitude is relatively small. This in turn increases phase noise of the oscillator due to a limited RF power of the generated carrier. When the negative conductance margin is excessive (with respect to the circuit losses), the oscillator signal becomes distorted before the signal amplitude reaches its limit. As with standard RF oscillator designs, margin of 2 is a practical choice between available RF power and signal distortion.

D. Phase noise

Phase noise of self-oscillating active inductor can be modeled using LTI (linear time invariant) method used previously by Razavi [6] for ring oscillators and Cranickx [7] for standard gyrator resonators. Although less accurate than LTV (linear time variant) method of Hajimiri and Lee [8], it allows for a much quicker estimation of phase noise performance of the presented oscillator.

In the proposed oscillator, each noise source contributes to $S_{out}(\omega_m)$, the output noise power spectral density (PSD). Three main sources are: transconductance amplifiers and the phase shifter resistor R_{out}. All sources are assumed to be uncorrelated and, to simplify analysis, only thermal noise is considered. To calculate phase noise at frequencies ω_m close to the carrier, PSD of each of the noise sources is multiplied by the corresponding noise transfer function. In LTI approach these transfer functions are linearised around the carrier frequency using Taylor series [6]. The phase noise is

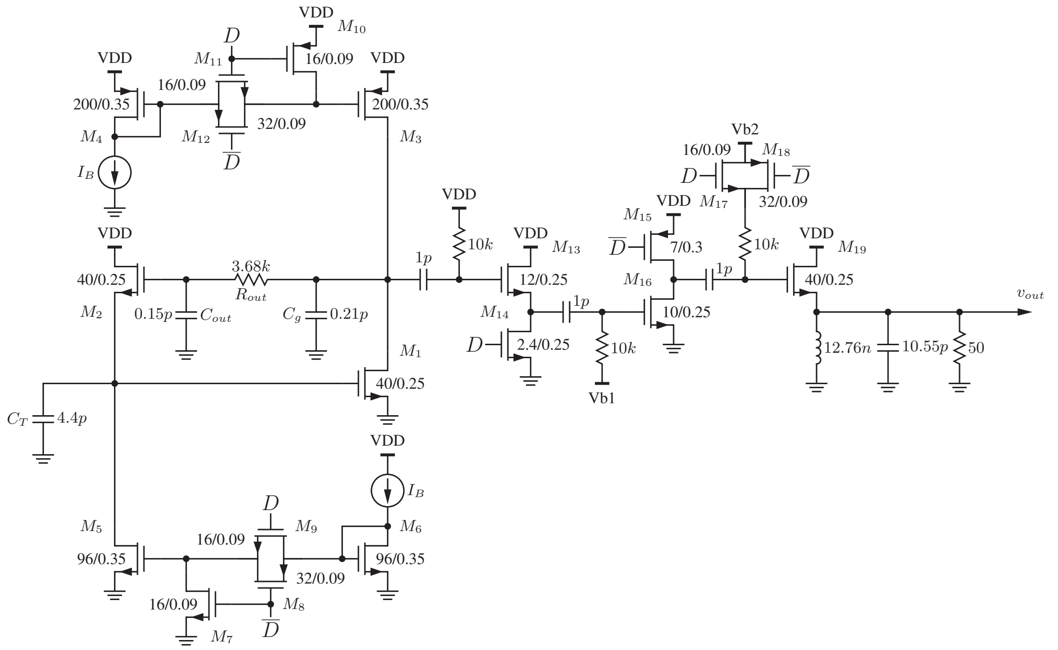

Fig. 3. Complete schematics of OOK transmitter.

then calculated using the formula for a normalised theoretical one-sided spectrum of oscillator signal [9]

$$L(\omega_m) = \frac{S_{out}(\omega_m)}{V_{out}^2/2} \tag{11}$$

where V_{out} is the amplitude of the oscillator signal. Note that the presented method accounts for a total noise i.e. phase and amplitude noise at offset frequency.

This methodology combined with the results of detailed noise analysis from our previous work [10] and model parameters from (1), the output noise PSD of a degenerated active inductor oscillator, at frequencies $\omega_m \ll \omega_0$ is given by

$$S_{out}(\omega_m) \approx \frac{kT\gamma}{\left(1 + \frac{C_T C_G}{gm_1 gm_2} \cdot \frac{\omega_0^4}{\omega_{z2}^2}\right)^2} \left[\frac{gm_2}{\omega_0^2 C_T^2} + \frac{1}{gm_1} + \right.$$
$$\left. + \frac{1}{gm_1^2 R_{out}} \left(1 + \frac{gm_1 gm_2}{\omega_0^2 C_T C_G}\right)^2\right] \cdot \frac{\omega_0^2}{\omega_m^2} \tag{12}$$

where k is Boltzmann's constant, T is temperature in Kelvins, γ is a process dependent noise constant. For the parameter values chosen for the design presented in this paper, estimated phase noise levels are in the range of -100 dBc/Hz at 1 MHz offset from 434 MHz carrier. In practice, the phase noise level will be worse, because the presented LTI model does not account for a time variant oscillator behavior or a non-linear noise conversion effects. Phase noise performance of degenerated active inductors is limited due to active circuits generating significant levels of noise and harmonic distortion bounding the available amplitude of oscillations.

III. Transmitter architecture

Fig. 3 depicts the proposed concept of the OOK transmitter designed using UMC 90 nm 1P9M RF process libraries. The circuit consists of three main components: bias network with switches, oscillator core and buffer amplifier with 50 Ω load. Note that most of the transistors used are not minimum size devices. This is because, firstly, in deep submicron RF process low gm to g_{ds} ratios reduce the available magnitude of negative resistance of the proposed oscillator. Secondly, a finer resolution of 90 nm CMOS, allows for more accurate dimensioning of larger devices.

A. Switched bias network

Switched bias network allows to turn on and off the oscillator core and the output buffer. The transmitter is modulated using binary signal and its negated version through the inputs D and $\overline{D}$, respectively. A standard 1:1 current mirror topology provides a constant bias current to the oscillator core. Transistors M_8, M_9, M_{11} and M_{12} are used as transmission gates that deliver DC voltage for M_3 and M_6 current sources, respectively. M_7 and M_{10} eliminate charge stored in parasitic capacitances during off period. Switches M_{14} and M_{15} act as active loads for the amplifiers, whereas M_{18} and M_{19} form switchable biasing network.

B. Oscillator core

Transistors M_1 and M_2 together with C_T, C_g, C_{out} and R_{out} form the self-oscillating, active inductor resonator. The oscillator can be tuned to the resonant frequency by changing the current mirrors bias source, I_B. All the resistors, including R_{out}, are a polysilicon resistors optimised for RF applications. All of the capacitors shown are high-Q MIM RF capacitors.

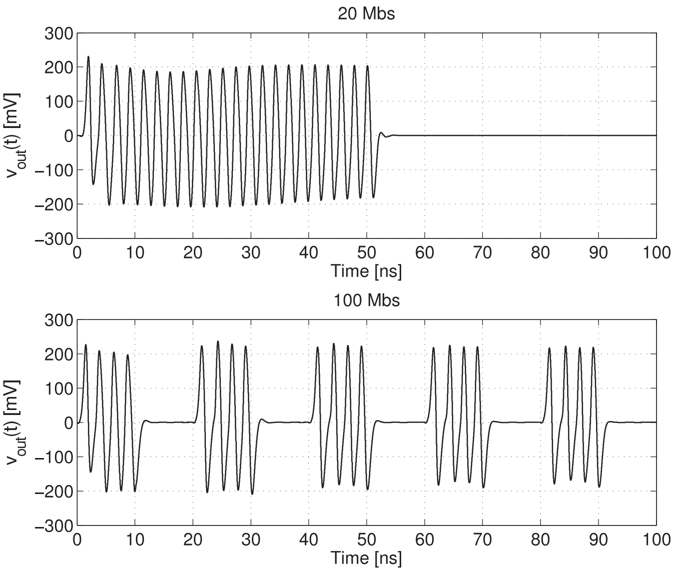

Fig. 4. Simulated output voltage for 20 Mbps and 100 Mbps modulation speeds.

Note that the output buffer is connected to the common source transconductor output to exploit larger signal amplitude swing at this point.

C. Output buffer

This subcircuit consists of three, class A stages for improved linearity. DC blocking capacitors of 1 pF were chosen to minimise time constants, allowing for faster transitions at the cost of a reduced output amplitude. The input amplifier is a common drain voltage follower, providing high impedance load to the oscillator core. Switch M_{14} acts as a linear resistor during On state, while the second stage compensates for losses in non-ideal source followers. This is a common source amplifier with switched PMOS linear resistor as a load. Finally, the output stage is a tuned voltage follower with passive LC tank to maximise voltage swing on a load resistor of 50 Ω. To avoid power dissipation due to a lossy inductor, its Q factor should be as large as possible. Particular values of LC tank components are trade-off between peaking due to a rapid switching, signal distortion and response time. Total voltage gain of the amplifier in this example is set to 0 dB to avoid an excessive distortion due to a large signal operation of the oscillator.

IV. Simulation results

The above circuit has been simulated in Eldo RF using transient and frequency steady state simulation with noise. The oscillator core has been analysed in terms of typical parameters: carrier frequency, tuning range and phase noise. For the bias currents of 700 µA delivered to each of the transconductors, the core produces sinusoidal oscillations at 433.7 MHz with an amplitude of 200 mV and an average start-up time of 3 ns. If necessary, the oscillator can be tuned from 382 MHz to 495 MHz using bias current source I_B. Phase noise at 1 MHz offset from 434 MHz signal reaches -93 dBc/Hz. The output amplifier allows delivery of -4 dBm of RF power to a 50 Ω load. Figure 4 presents the circuit response for square wave modulation signal with 50% duty cycle. Two modulation speeds were analysed: 20 Mbps and 100 Mbps.

Power consumption of the transmitter can be broken down into the following: 7.96 mW for the output, class A amplifier, 1.4 mW for the bias network and 1.4 mW for the oscillator core from a 1 V power supply. Note that power consumption of the core using the proposed resonator compensation method is only 13% of the total DC power necessary to operate.

V. Conclusion

In this paper we have presented the concept of OOK transmitter using a novel, power efficient self-oscillating CMOS active inductor. Design insights to a negative resistance generation mechanism in simple gyrators has been described together with simulation results of the complete transmitter architecture. The proposed circuit supports fast modulation signals up to 100 Mbps with equivalent phase noise performance of circuits using active inductor resonators.

Acknowledgments

Research presented in this paper was funded by CTVR, The Telecommunication Research Centre (SFI 03/CE3/I405) by Science Foundation Ireland under the National Development Plan. The authors gratefully acknowledge this support. Also authors would like to thank Dr. A. Keady for a valuable discussion on switching circuits and OOK performance.

References

[1] P. Quinlan, P. Crowley, M. Chanca, S. Hudson, B. Hunt, K. Mulvaney, G. Retz, C. E. O'Sullivan, and P. Walsh, "A multimode 0.3-200-kb/s transceiver for the 433/868/915-MHz bands in 0.25-um CMOS," *IEEE Journal of Solid-State Circuits*, vol. 39, no. 12, pp. 2297–2310, 2004.

[2] J. Ryu, M. Kim, J. Lee, B.-S. Kim, M.-Q. Lee, and S. Nam, "Low power OOK transmitter for wireless capsule endoscope," in *Microwave Symposium, 2007. IEEE/MTT-S International*, Honolulu, HI, 2007, pp. 855–858.

[3] F. Zhao, X. Gao, H. Zhang, K. Hu, and Z. Hong, "A CMOS 434/868 MHz FSK/OOK transmitter with integrated fractional-n PLL," in *Wireless and Microwave Technology Conference, 2009. WAMICON '09. IEEE 10th Annual*, Clearwater, FL, 2009, pp. 1–4.

[4] K. W. Moulding and G. A. Wilson, "A fully integrated 5 gyrator filter at video frequencies," in *Solid State Circuits Conference ESSCIRC '77. 3rd European*, Ulm, F.R. Germany, 1977, pp. 148–151.

[5] Y. T. Wang and A. A. Abidi, "CMOS active filter design at very high frequencies," *IEEE Journal of Solid-State Circuits*, vol. 25, no. 6, pp. 1562–1574, Dec. 1990.

[6] B. Razavi, *RF Microelectronics*. Upper Saddle River, NJ, USA: Prentice-Hall, Inc., 1998.

[7] J. Craninckx and M. Steyaert, "Low-noise voltage-controlled oscillators using enhanced LC-tanks," *IEEE Transactions on Circuits and Systems II: Analog and Digital Signal Processing*, vol. 42, no. 12, pp. 794–804, Dec. 1995.

[8] T. H. Lee and A. Hajimiri, "Oscillator phase noise: a tutorial," in *Solid-State Circuits, IEEE Journal of*, vol. 35, no. 3, San Diego, CA, 2000, pp. 326–336.

[9] F. Gardner, *Phaselock techniques*. New York: John Wiley & Sons, 1979.

[10] G. Szczepkowski and R. Farrell, "Noise and dynamic range of CMOS degenerated active inductor resonators," in *Circuit Theory and Design, 2009. ECCTD 2009. European Conference on*, Antalya, Aug. 2009, pp. 595–598.